MATTHIAS FENGLER, WOLFGANG HÄRDLE AND PETER SCHMIDT

COMMON FACTORS GOVERNING VDAX MOVEMENTS AND THE MAXIMUM LOSS

Matthias Fengler (fengler@wiwi.hu-berlin.de) and Wolfgang Härdle,
Humboldt-Universität zu Berlin, Wirtschaftswissenschaftliche Fakultät,
Institut für Statistik und Ökonometrie,
Center for Applied Statistics and Econometrics (CASE),
Spandauer Strasse 1, D - 10178 Berlin.
Peter Schmidt (Peter.Schmidt@ib.bankgesellschaft.de),
Bankgesellschaft Berlin, Quantitative Research,
Alexanderplatz 2, D - 10178 Berlin
The authors thank two anonymous referees for helpful suggestions.
The research for this paper was supported by the
Sonderforschungsbereich 373 at the Humboldt-Universität zu Berlin.
We gratefully acknowledge the support of the
Deutsche Forschungsgemeinschaft.

1. Introduction

Pricing options and the estimation of real volatility of the underlying asset have an intimate relationship. A number of approaches based on the geometric Brownian motion, e.g. the BLACK and SCHOLES (B&S) model, yield explicit analytical formulas of the option price which depends on the parameters characterising the option and the volatility parameter of the underlying price process. In the particular B&S case, the volatility parameter σ is a constant across all maturities τ and strike prices K. However, when using quoted option prices to estimate the volatility parameter from the B&S option pricing formula, one observes a time-varying, pronounced term structure of so called implied volatilities. Monitoring the dynamics of this volatility term structure is an important element of analysis and prediction for many financial applications such as trading, hedging and risk management, see TALEB (1997).

The objective of our paper is to identify common factors of implied volatility movements of "at the money" options on the German stock index DAX from 18/03/96 to 19/12/97. Identifying common factors is important from the perspective of risk management, vega-hedging and volatility trading. A natural technique to identify the number of stochastic shocks that move the implied volatility surface is principal components analysis (PCA), SKIADOPOULOS, HODGES and CLEWLOW (1999), ALEXANDER (2001), FENGLER, HÄRDLE and VILLA (2001). With respect to risk management, PCA has the advantage that the complete term structure can be represented by a small number of variables, i.e. the dimension of the risk factor space can be drastically reduced.

Our analysis indicates that two risk factors explain a large proportion of total variation in the term structure of "at the money" DAX options. Building on this result, we present a risk management tool based on the maximum loss (ML) methodology. We also provide an intui-

tive meaning of the identified factors and consider their stability over time.
The paper is organised as follows: In the next section we present the data and necessary cleaning and correction algorithms. In section 3 we perform the PCA procedure and identify the dominant risk factors. Section 4 discusses the stability of our analysis over time. In section 5 the ideas are applied to ML methodology, while section 6 provides an intuitive example. Section 7 concludes.

2. Data Description

The subject of investigation here is implied volatility as measured by the German VDAX subindices available from Deutsche Börse AG. These indices, representing different option maturities from one to 24 months, measure volatility implied in European-style calls and puts with strikes equal to the current DAX level, i.e. the options are "at the money" (ATM). The index calculations are based on the assumption that the Black & Scholes (B&S) option pricing formula is a suitable model for the valuation of option prices. The B&S formula for a European call at time t, C_t, is

$$C_t = S_t \Phi(d_1) - K e^{-r\tau} \Phi(d_2)$$

where $\Phi(x)$ denotes the cumulative distribution function of a standard normal random variable and the coefficients are given by

$$d_1 = \frac{\left[\ln\left(\frac{S_t}{K}\right) + \left(r + \frac{1}{2}\sigma^2\right)\tau \right]}{\sigma\sqrt{\tau}}; \; d_2 = d_1 - \sigma\sqrt{\tau}$$

Here r denotes the risk-free interest rate, S_t the price of the underlying asset, $\tau = T - t$ time to maturity and K the strike price. For ATM options the strike is $K = S_t$.

The only parameter in the B&S formula that cannot be observed directly is the actual volatility σ of the underlying price process. One may substitute for σ an estimate based on prior observed returns of the underlying asset. An alternative approach uses *implied* volatilities. The implied volatility is defined as the parameter $\hat{\sigma}$ that yields the actually observed market price of a particular option when substituted into the B&S formula. Quoting option prices in terms of implied volatilities does not necessarily mean that market participants assume that the B&S formula is a valid model for the market. Instead they use this formula as a convenient way of describing and quoting option prices via implied volatilities.
Implied volatilities can be calculated by iterative numerical techniques and may be used to monitor the market's opinion about the volatility of a particular price process. The implied B&S volatility is not equal to the actual volatility σ but may reflect in some way the expectations of market participants with respect to the future volatility of the underlying price process. Nevertheless, the links between actual and implied volatilities depend on the theoretical assumptions of the particular model assumed and can be of complex nature. For theoretical approaches of that kind we refer e.g. to SCHÖNBUCHER (1999).
The options on the DAX are the most actively traded contracts at the German-Swiss derivatives exchange EUREX. Implied volatility estimates for ATM DAX options may be obtained from Deutsche Börse AG, which has been delivering daily closing prices of VDAX subindices for maturities of 1, 2, 3, 6, 9, 12, 18 and 24 month since 18/03/96. On this day trading in long term options started at EUREX.
VDAX subindices for our analysis were received from Deutsche Börse AG for the data period covered. Interest rate data, i.e. the 3 and 6 month FIBOR, and the DAX closing notation are provided by Thompson Financial

Figure 1: Term Structure of ATM DAX Implied Volatilities: 31/10/97 (Solid), 03/11/97 (Dotted), 17/11/97 (Dashed) and 20/11/97 (Dotted and Dashed)

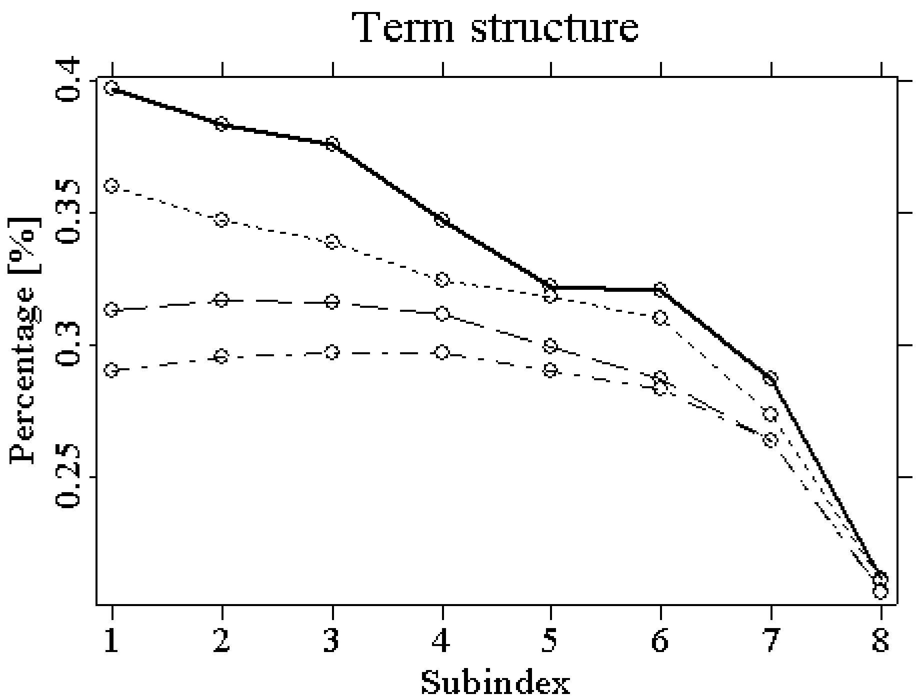

Datastream. The term structure for ATM DAX options can be derived from VDAX subindices for any given trading day. Typical shapes are plotted in Figure 1.

If we compare the volatility structure of 31/10/97 (solid line) with that of 03/11/97 (dotted line), we observe an downward shift in the levels of implied volatilities. Moreover, both plots display an inversion as short term volatilities are higher than long term ones. Only a couple of weeks later, on 17/11/97 (dashed line) and 20/11/97 (dotted and dashed line), the term structure had returned to lower levels. Evidently, during the market tumble in fall of 1997, the ATM term structure shifted and changed its shape considerably over time.

VDAX calculations are based on the inversion of the B&S formula. For a given subindex, implied volatility is estimated from a subset of liquid "near the money" options. The contribution of each implied volatility estimate is not subject to an explicit weighting scheme. Instead, weights are determined implicitly by an ordinary least squares regression yielding an estimate of ATM implied volatility. For detailed information on the VDAX calculation method see REDELBERGER (1994).

We do not exclusively confine our analysis to the highly liquid short term option contracts which are represented by the subindices 1 to 4. This is done for two reasons: First, limited trading occurs on certain days in longer term contracts, thus there might be information in

these data entries on those days. Ignoring them completely bears the risk of losing information. Second, we need a constant option maturity instead of floating targets based on EUREX expiration dates. This is vital because changes in volatility arising from changing option maturities (due to the passage of time) will affect the statistical analysis. Thus we need longer term contracts to calculate volatility indices with constant maturities, which is most important for short-dated options. To accomplish constant time to maturity we linearly interpolate between neighbouring VDAX subindices.
With $\hat{\sigma}_t(\tau_-)$ and $\hat{\sigma}_t(\tau_+)$, the respective nearby and second nearby implied volatility subindices, we calculate indices $\hat{\sigma}_t(\tau_j^*)$ with fixed maturities of τ_j^* = 30, 60, 90, 180, 270, 360, 540, 720 calendar days by

$$\hat{\sigma}_t(\tau^*) = \hat{\sigma}_t(\tau_-)\left[1 - \frac{\tau^* - \tau_-}{\tau_+ - \tau_-}\right] + \hat{\sigma}_t(\tau_+)\left[\frac{\tau^* - \tau_-}{\tau_+ - \tau_-}\right]$$

Proceeding this way, we obtain j = 8 time series of fixed maturity. Each time series is a weighted average of two neighbouring maturities and contains n = 441 data points of implied volatilities. From now on we will refer to fixed maturity when dealing with VDAX indices.

3. Principal Components Analysis of Implied Volatility Dynamics

In this section we outline a procedure to extract common factors from historical term structure movements that govern the actual dynamics of implied volatilities. The basic data set for our analysis is a collection of term structures like in Figure 1. In order to identify common factors we use principal components analysis (PCA). Changes in the term structure can be decomposed by PCA into a set of factors constituting an orthogonal base.
We compute augmented DICKEY-FULLER (ADF) tests on daily implied volatility indices $\hat{\sigma}_t(\tau_j^*)$. The ADF tests show that the null hypothesis of instationarity cannot be rejected for any VDAX-subindex even at the 10% level. level. Our results suggest to perform principal components analysis on the returns $x_{jt} = \left(\frac{\hat{\sigma}_t(\tau_j^*)}{\hat{\sigma}_{t-1}(\tau_j^*)}\right) - 1$ of implied volatility indices.
These returns seem to be stationary as an additional ADF analysis indicates.
Sample means of the returns x_{jt} are very close to zero and hence of negligible size. Table 1 shows the sample correlation matrix of x_{jt}. Note that sample correlations are considerably

Table I: Sample Correlations of Implied Volatility Returns

Sub 1	Sub 2	Sub 3	Sub 4	Sub 5	Sub 6	Sub 7	Sub 8
1.00	0.73	0.70	0.72	0.61	0.44	0.34	0.27
	1.00	0.89	0.75	0.70	0.47	0.28	0.29
		1.00	0.81	0.72	0.50	0.32	0.24
			1.00	0.82	0.54	0.49	0.30
				1.00	0.55	0.46	0.31
					1.00	0.38	0.24
						1.00	0.28
							1.00

smaller for longer option maturities than for the shorter ones. This may be due to market segmentation: Short term contracts are most heavily traded by professional traders whereas longer maturities are rather illiquid and may be used by long term hedgers and investors in the first place, see TALEB (1997).

PCA is performed by decomposing the empirical covariance matrix Ω into the Jordan Canonical Form $\Omega = \Gamma^{Tr}\Lambda\Gamma$, where Λ is an 8 x 8 diagonal matrix of eigenvalues λ_k, k = 1,2,...,8 and $\Gamma = (\gamma_1, \gamma_2, \ldots, \gamma_8)$ an 8 x 8 matrix of eigenvectors γ_k. Time series of principal components are obtained by $Y = X\,\Gamma$. X denotes the 441 x 8 matrix of implied volatility returns and Y is the 441 x 8 matrix of principal components.

A measure of how well the first p principal components explain variation in the underlying data is given by the relative proportion of eigenvalues:

$$\zeta_p = \frac{\sum_{k=1}^{p\le 8} \lambda_k}{\sum_{k=1}^{8} \lambda_k} = \frac{\sum_{k=1}^{p\le 8} \mathrm{Var}\,(y_k)}{\sum_{k=1}^{8} \mathrm{Var}\,(y_k)}.$$

Figure 2 shows the proportion of variance (dashed line) and the cumulative proportion of variance ζ_p explained by the respective number of principal components (solid line).

As is evident from Figure 2, the first PC captures 73.5% of the total data variability. The second PC captures an additional 9.9% of total variance. The other PCs explain a considerably smaller amount of variation in implied volatility returns. Thus the two dominant PCs cumulatively explain around 83.4% of total variance in ATM volatilities for DAX options.

Figure 2: Variance Explained by k = 1,2,...,8 Principal Components

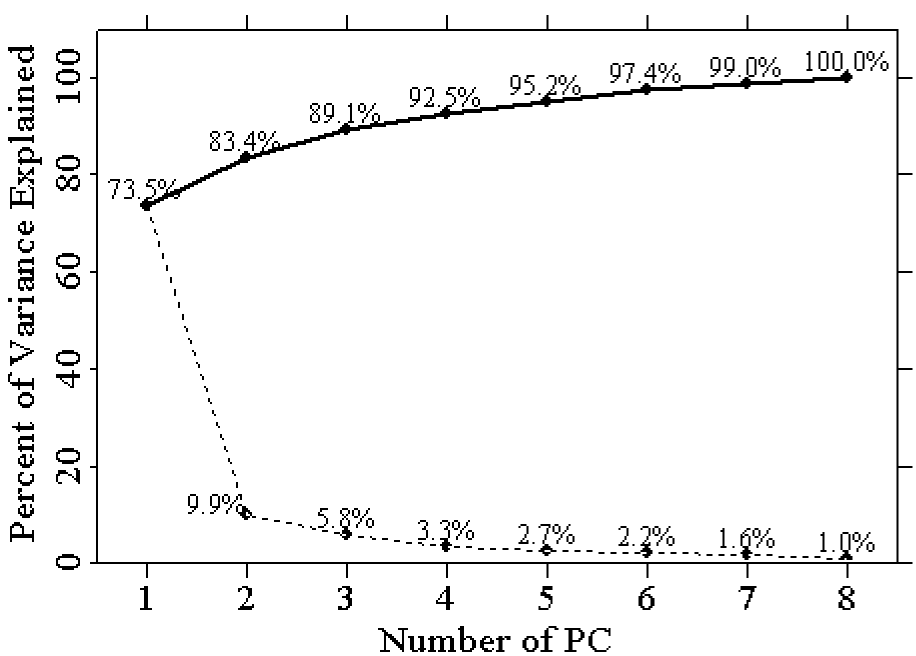

As is also clear from Figure 2, the "variance explained" plot exhibits an "elbow-like" shape at the second PC. The so called "elbow criterion" suggests to retain the first two components here. The remaining residual information may be interpreted as random noise. Hence, keeping two factors, we may use the following representation for implied volatility returns:

$$x_{jt} = \sum_{k=1}^{2} \gamma_{jk} y_{kt} + \varepsilon_{jt},$$

where ε_{jt} is an i.i.d. nuisance term.

Figure 3 presents the factor loadings for the first two PCs. Obviously, a shock on the first factor tends to affect all maturities in a similar manner, causing a non-parallel shift. A shock in the second factor has a strong positive impact on the front maturity but a negative impact on the longer ones, thus causing a change of the slope in the term structure of implied volatilities. Similar results have been obtained by SKIADOPOULOS, HODGES and CLEWLOW (1999) for options on the S&P 500, SYLLA and VILLA (2000) on the CAC 40, and ALEXANDER (2001) on the FTSE 100. FENGLER, HÄRDLE and VILLA (2001) and CONT and FONSECA (2002) take a more comprehensive view on the whole implied volatility surface, but still, results follow the patterns discussed above.

4. Stability Analysis

In this section, we investigate the stability of our principal components analysis. If PCs are not stable over time due to changing volatility regimes, adaptive methods may further en-

Figure 3: Factor Loadings for the First and the Second Principal Component

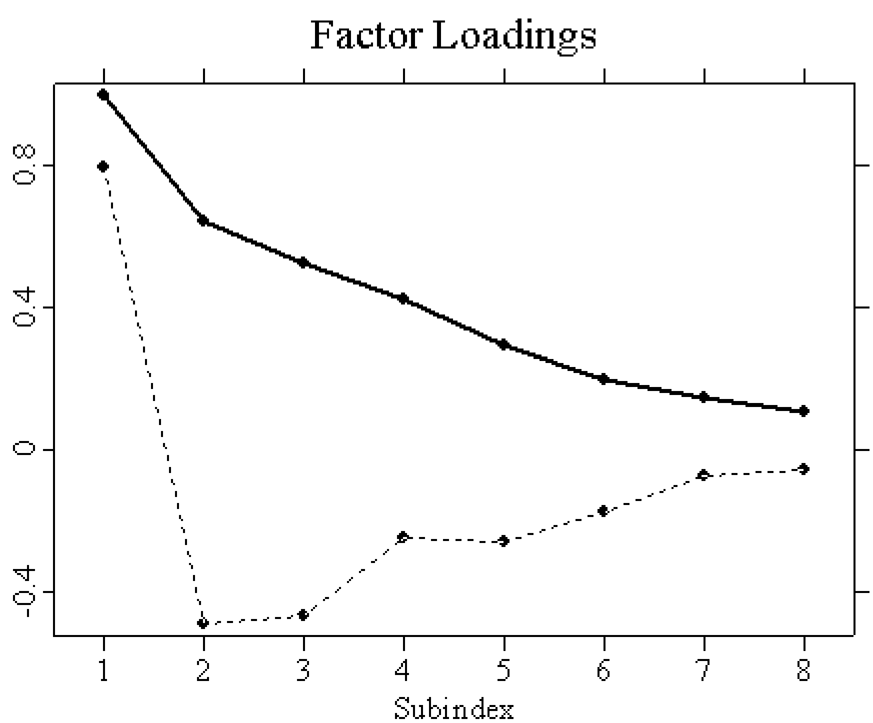

hance the accuracy of our procedures with respect to risk management applications.

Our stability analysis extends in two directions: First, daily data may be noisy because traders often consider different sections of the DAX ATM options implied volatility vector as distinct from each other, sometimes updating option quotes in the more liquid shorter maturities while ignoring the longer ones. Sections of the DAX options market with little or no order flow during the day thus may include stale data during and possibly at the end of the trading day. We estimate principal components using weekly data rather than daily. If PCs are stable, one would not expect to find substantially different results with daily versus weekly data.

Second, we divide our data set into $l = 1, 2$ non-overlapping periods of equal length. Each period contains m = 220 daily observations of first differences of implied VDAX subindices. As a common method (HÄRDLE and SIMAR, 2002), we conduct pairwise tests of $\lambda_{k,l}$ to see if the eigenvalues change significantly over time.

As is clear from Table 2, the in-sample proportion of variance explained by the first two PCs is slightly higher in weekly data compared to daily returns. This is not surprising since one would expect fewer unsystematic volatility movements in (higher quality) weekly data. In fact, weekly results are qualitatively very similar to daily ones, so we do not discuss them further here.

As can be seen from Table 2, the proportion of daily data variability explained by the first two PCs diminishes over the second subperiod. In order to test for the stability of the principal components over time we compute eigenvalues for both subperiods. A two-sided confidence interval for some pair of eigenvalues is given by

$$\ln\lambda_{k,1} - 2q_\alpha\sqrt{\frac{1}{m-1}} \le \ln\lambda_{k,2} \le \ln\lambda_{k,1} + 2q_\alpha\sqrt{\frac{1}{m-1}},$$

where q_α denotes the α-quantile of a standard normal distribution. We immediately have

$$\left|\ln\lambda_{k,1} - \ln\lambda_{k,2}\right| \ge 2q_\alpha\sqrt{\frac{1}{m-1}}$$

as a two-sided test for $H_0 : \lambda_{k,1} = \lambda_{k,2}$, i.e. equality of eigenvalues in both subperiods. The null hypothesis would be rejected if the above expression holds for the significance level chosen.

Critical values for the null hypothesis are 0.222 (10%), 0.265 (5%) and 0.348 (1%). The estimated absolute log-differences for the pair of eigenvalues $\lambda_{1,1}$, $\lambda_{1,2}$ and $\lambda_{2,1}$, $\lambda_{2,2}$ are 0.667 and 1.183 respectively, and hence are both significant different from zero at the 1% level. This indicates that the common factors governing implied volatility movements measured by the German VDAX may vary over time. With respect to this finding, adaptive estimation techniques such as proposed by HÄRDLE, SPOKOINY and TEYSSIERE (2000) may effectively be employed in an analysis of similar

Table 2: Principal Components Analysis: Cumulative Percentages of Variance Explained

PC No.	1	2	3	4	5	6	7	8
Weekly: 18/03/96–19/12/97	71.10%	86.35%	92.00%	95.09%	96.74%	98.09%	99.15%	100%
Daily: 18/03/96–19/12/97	73.50%	83.40%	89.10%	92.50%	95.20%	97.40%	99.00%	100%
Sub 1: 18/03/96–05/02/97	83.64%	92.87%	95.12%	96.82%	97.92%	98.82%	99.58%	100%
Sub 2: 05/02/97–19/12/97	68.26%	79.05%	86.27%	90.67%	94.34%	96.81%	98.79%	100%

kind. We further discuss the stability of our analysis in section 6.

5. Measuring ATM Implied Volatility Risk by Maximum Loss

One key issue in portfolio management is the measurement of a portfolio's inherent market risk. Monte-Carlo simulation techniques may be used to assess the risks of highly non-linear portfolios such as option portfolios. Unfortunately these techniques are computationally expensive and time consuming. In this section we introduce an approach to approximate the maximum loss of delta-gamma hedged option portfolios analytically.

The market value P of a portfolio consisting of w single options on the same asset is susceptible to changes in interest rates, to the price of the underlying asset, to the passage of time and to the different implied volatilities contained in the portfolio. The Taylor series expansion of the change in portfolio value from time t – 1 to time t is

$$\Delta P_t \approx \sum_{u=1}^{w}\left[\frac{\partial O_{ut}}{\partial \sigma_t(\tau_u)}\Delta\sigma_t(\tau_u)+\frac{\partial O_{ut}}{\partial t}\Delta t+\frac{\partial O_{ut}}{\partial r_t}\Delta r+\frac{\partial O_{ut}}{\partial S_t}\Delta S_t+\frac{1}{2}\frac{\partial^2 O_{ut}}{\partial S_t^2}(\Delta S_t)^2\right], \quad (1)$$

where O_{ut} denotes the option price with the option specific maturity τ_u at time t. Interest rates r may well be assumed to be constant over short investment periods, i.e. we can ignore the interest rate sensitivity of the portfolio in our analysis.

As a common practice traders directly trade the so called vega of their portfolios, which is the portfolio sensitivity to implied volatility. For European-style options on an underlying asset vega can be derived by differentiating the B&S formula with respect to σ. In order to establish vega trades, market professionals use delta-gamma neutral hedging strategies which are insensitive to changes in the underlying asset and to time decay, see TALEB (1997).

A popular strategy to exploit relative term structure movements is buying and selling straddles of different option maturities at the same time. A straddle consists of the same number of ATM calls and puts. For instance, when a trader expects the short term implied volatilities to fall relative to the long term ones, he will sell straddles in short term contracts and simultaneously buy straddles in longer maturities. The resulting portfolio will be delta-gamma neutral and nearly theta-neutral over short periods of time (i.e. nearly insensitive to time decay on a day-by-day basis). In this case, the Taylor expansion simplifies to

$$\Delta P_t \approx \sum_{u=1}^{w}\left[\frac{\partial O_{ut}}{\partial \sigma_t(\tau_u)}\Delta\sigma_t(\tau_u)\right]. \quad (2)$$

Thus the dominant determinants of changes in portfolio value are implied volatilities. Principal components analysis allows us to write the returns of the implied volatilities $\hat{\sigma}_t(\tau_u)$ as a linear combination of PCs. Thus, taking the respective nearby fixed maturity subindex $\hat{\sigma}_t(\tau_j^*)$ as a proxy for $\hat{\sigma}_t(\tau_u)$, we get

$$\Delta P_t \approx \sum_{u=1}^{w}\left[\frac{\partial O_{ut}}{\partial \sigma_t(\tau_u)}\left(\sum_k \gamma_{jk}\, y_{kt}\right)\hat{\sigma}_{t-1}(\tau_u^*)\right] \quad (3)$$

Starting from equation 3 we now present a concept for risk management using the concept of maximum loss (ML) based on principal components.

ML analysis is based on the probability distribution of a change in the value of a portfolio attributable to a change in fundamentals over a short period of time. Since implied volatilities fundamentally determine the prices of delta-gamma hedged derivatives portfolios, we require an accurate characterisation of the future probability distribution of volatilities of various-maturity options portfolios.

Maximum loss is defined as the maximum possible loss

- over a given risk factor space A_τ, where A_τ will be assumed a closed set with confidence level $\Pr(y|y \in A_\tau) = \alpha$
- for some holding period τ.

In order to maintain delta-gamma neutrality, dynamic hedgers usually revise their derivatives portfolios after short periods of time. $\tau = t - (t-1)$ may be a realistic assumption from a practitioner's point of view, which implies a portfolio revision on every single trading day.

At first glance, the ML-definition has the same appearance as the well known value at risk (VaR) definition. There is an important difference, however: Whereas VaR calculation requires the profit and loss distribution to be known, ML is defined in the risk factor space, see STUDER (1995).

In our analysis we decomposed the term structure of implied volatilities into a set of two principal components that explains an essential part of term structure variation. Hence, we use only the first two PCs as risk factors in our empirical analysis in section 6. In order to construct the profit and loss surface on A_τ, the whole option portfolio has to be priced for each point in the factor space. This is approximated by marking the portfolio to the market at discrete points $y_i \in A_\tau$. The particular scenario in A_τ where the maximum loss would occur is called the ML scenario.

Assuming multinormally distributed PCs, trust regions can be constructed using the joint density function

$$\varphi_\tau(y) = \frac{1}{(2\pi)^{1/2}\sqrt{\det \Lambda_2}} \exp\left(-\frac{1}{2} y^{Tr} \Lambda_2^{-1} y\right),$$

where the matrix Λ_2 is a 2 x 2 diagonal matrix of eigenvalues λ_k, k = 1,2 and $y = (y_1, y_2)$. $y^{Tr}\Lambda_2^{-1}y$ results in a random variable which is chi-square distributed with 2 degrees of freedom. Hence, a valid trust region for our portfolio is obtained by the equation for a centered ellipse $A_\tau = \left(y | y^{Tr}\Lambda_2^{-1} y \le c_\alpha\right)$, where c_α denotes the α-quantile of a chi-squared distribution with 2 degrees of freedom.

6. An Empirical Example: Assessing Term Structure Portfolio Risk

For illustration, we consider a strategy which aims at exploiting relative changes in the term structure of implied volatilities, i.e. at decreasing short term and rising long term volatility. Belonging to the class of strategies where the vega exposure of the portfolio contributes overwhelmingly to its overall risk structure, it is sufficiently complex for meaningful computations of ML, yet at the same time simple enough to yield easily interpretable results. In a first step, we give a static analysis of the ML of the portfolio for a number of trading days, and then a summarizing report on the entire sample period.

Consider the following portfolio whose one-day ML will be of interest: Sell an ATM call and an ATM put with 3 months maturity and buy an ATM call and an ATM put with 6 months maturity, i.e. sell a 3-months straddle and buy the 6-months one (actually, in our computations we use 100 options each). Clearly, this strategy can be considered delta-gamma-neutral. Moreover, as theta and rho risks of these two straddles are of opposite sign, they partially counterbalance each other. Therefore, the remaining risks are small enough to be negligible over the daily time horizon under consideration, and the first order Taylor expansion, Equation (1), can be reduced to the terms incorporating vega risks

Figure 4: Critical Volatility Scenarios on 29/03/96 (Ellipse), Current Volatility Level (Circle) and ML Scenario (Filled Circle); Compare with Figure 5 and Table 3

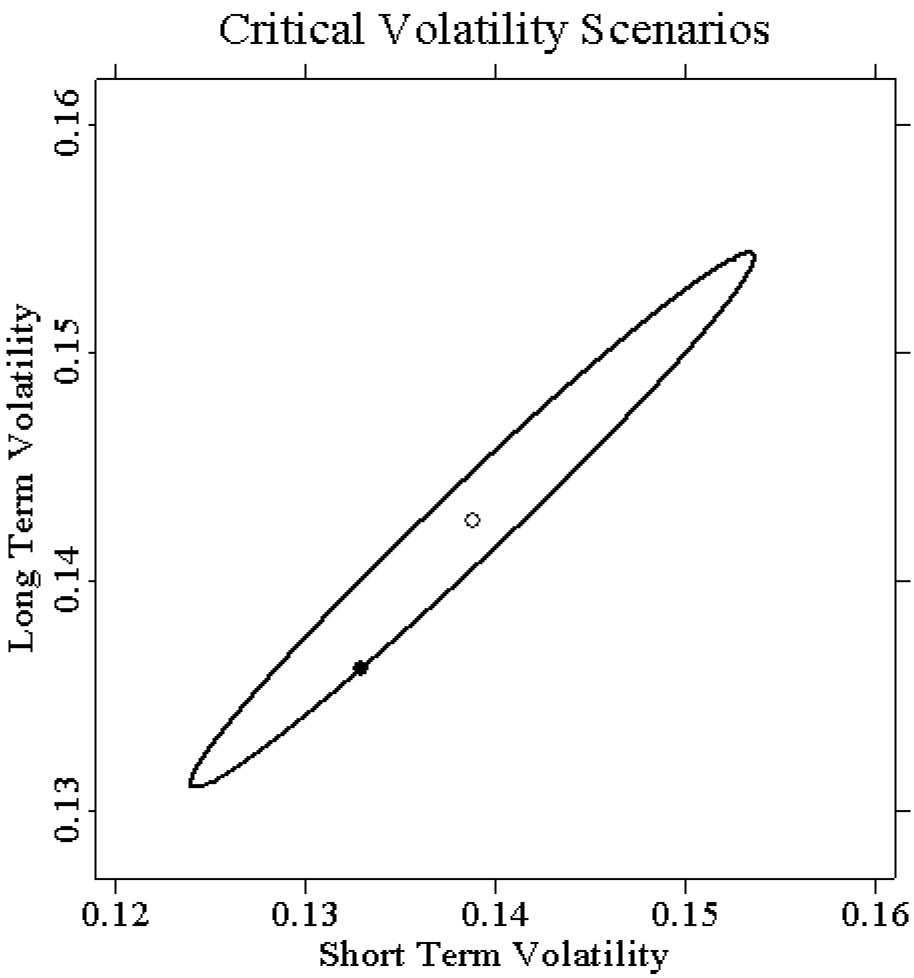

only, Equation (2). We further simplify the setting by assuming that for each t and any value S_t of the DAX index ATM options of 3 and 6 months maturity to be available, i.e. $K = S_t$. This portfolio is created in time t, priced under the assumptions of the B&S model with no dividends at the actual realizations of S_t, r_t and the volatility vector σ_t, and held until t + 1, where t = 1, ... T – 1 = 440. Note that our analysis is focussed on ML only, i.e. we do not consider the risks and rewards of this position from a trader's point of view.

The assessment of the one-day ML follows the lines laid out above and was implemented in XploRe, see HÄRDLE, KLINKE, MÜLLER (2000): We model two risk factors which contribute for approximately 83% of overall variance to implied volatility returns and choose an $\alpha = 99\%$ confidence level for the trust region A_1. Hence the critical range of risk factors can be found along the perimeter of the corresponding ellipse $A_1 = (y|\ y^{Tr}\Lambda y = c_\alpha)$, where c_α denotes the α-quantile of the chi-squared distribution with 2 degrees of freedom. Contrary

Figure 5: Critical Volatility Scenarios (Gray Ellipse), Portfolio Changes (Black Ellipse, Gains Solid Line, Losses Dashed) and the ML (Black Ball) on 29/03/96; Compare with Figure 4 and Table 3

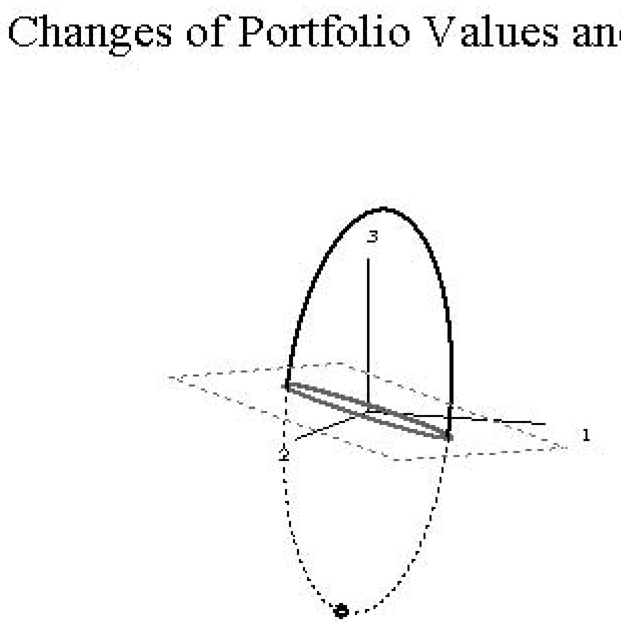

to more complex portfolios and scenarios, where the ML may well lie within the trust region A_τ, in our case critical scenarios can only occur along its perimeter due to the monotonicity of the portfolio's risk structure in the two factors. It is hence only there where we need to price the portfolio. The ellipse is discretised on a dense grid $y = (y_1,y_2)$ of 100.000 points in order to receive a sufficiently precise estimate of potential scenarios and transformed into the space of volatility returns by $x = y\ (\gamma_1,\gamma_2)^{Tr}$, where (γ_1,γ_2) is the 8x2 matrix of the two eigenvectors corresponding to the first two biggest eigenvalues. The volatility returns corresponding to the 3 and 6 month implied volatilities are multiplied to the current volatility scenario and displayed to illustrate the situation of 29/03/96 in Figure 4.

The extremely narrow shape of the ellipse in Figure 4 reflects the results which we have already commented above: Shifts of the same sign both in short and long term volatilities account for 73.5% of the shocks (the first factor), whereas slope shocks of different signs contribute only 9.9% to volatility movements (second factor). The maximum loss (filled circle) is found in the lower left quadrant to the current volatility levels (circle), i.e. when the long term volatility moves exactly against our bet. Figure 5 additionally displays the portfolio changes associated with the ellipse of critical volatility scenarios: Portfolio changes form an ellipse as well, and ML is marked by the black ball.

Table 3 gives an overview of scenarios which occurred during the sample period. Generally we observe that negative volatility returns in

Table 3: ML Scenarios for a Selection of Trading Days in 1996/97

Date	Initial Scenario		ML Scenario					
	Sub 3	Sub 4	Sub 3	Sub 4	Delta Sub 3	Delta Sub 4	ML	relative ML
29/03/96	13.88%	14.27%	13.30%	13.62%	–0.0058	–0.0065	–316.73	–5.02%
31/10/97	37.52%	34.67%	37.98%	34.48%	0.0046	–0.0019	–1076.90	–6.39%
03/11/97	33.85%	32.44%	33.56%	31.75%	–0.0029	–0.0069	–1029.50	–5.69%
17/11/97	31.60%	31.15%	30.85%	30.14%	–0.0075	–0.0101	–1002.60	–5.38%
20/11/97	29.66%	29.72%	28.72%	28.58%	–0.0094	–0.0114	–1007.00	–5.27%

the long term contract produce such a strong impact that gains in the short volatility position are compensated: On 29/03/96 (see Figures 4 and 5), at a drop of 0.65 percentage points of the 6-months implied volatility in conjunction with a 0.58 percentage points decrease in the 3-months contract the ML scenario occurs, which comes close to a level shift in implied volatilities (perfect level shifts occur at the vertices of the ellipse). Relative ML, defined as the ML divided by the initial portfolio value, is around 5.0%. We report relative ML, since the value of our position is homogenous of degree one in the level of the underlying asset, and the high ML in the second half of the sample period can largely be attributed to higher DAX levels. As can be seen, the general pattern discussed for 29/03/96 does not change: The high vega sensitivity of the 6-months contract is sufficiently large to dominate the ML scenarios. This pattern changes only marginally with higher volatility levels. On 31/10/97, however, during the crash period in the Asian crisis, when the term structure inverted significantly, the ML scenario corresponds to an even stronger inversion of the term structure. This is due to the decreasing relative vega sensitivity between short and long term options at high volatility levels.

Figure 6 shows a time series plot of the one-day relative ML, assuming that a new straddle portfolio is created in each t and held until t + 1. Additionally, the time series of the two implied volatility subindices and the underlying index (relative ML and DAX have been rescaled) are displayed in this figure. Relative ML is 4.9% at the minimum and 6.4% at the maximum, but as can be seen from Figure 6, it is not easy to separate the impact of volatility level changes on the one hand and the relative term structure movements on the other hand. It appears, however, that relative ML is increasing with higher volatility levels, which can be seen best during the fourth quarter 1996 when the market regime switches – in DERMAN's (1999) terminology – from a range-bounded to a stable trending market. Volatility term structure effects are visible during the crash period in the fourth quarter 1997, when strong term structure inversions occur (the thin black line, i.e. 3-months subindex is above the 6-months subindex, the thin gray line). Precisely this susceptibility to changes in the market environment make ML a suitable risk management tool for the given context.

One remark with respect to the actual confidence level seems to be necessary: Although we used a 99% quantile to compute the risk factors it should be kept in mind that this is not the true confidence level of the ML, as by the risk factors only 83.4% of the in-sample variance of implied volatility returns is explained. The true level of confidence can be found by Monte Carlo simulation techniques, which is beyond the scope of this paper. Given that Monte Carlo simulations are usually not

Figure 6: Implied 3 and 6 Months Implied Volatility (Thin Black and Gray Lines) and Relative ML*10 (Thick Black Line), and DAX $*10^{-4}$ (Dashed).

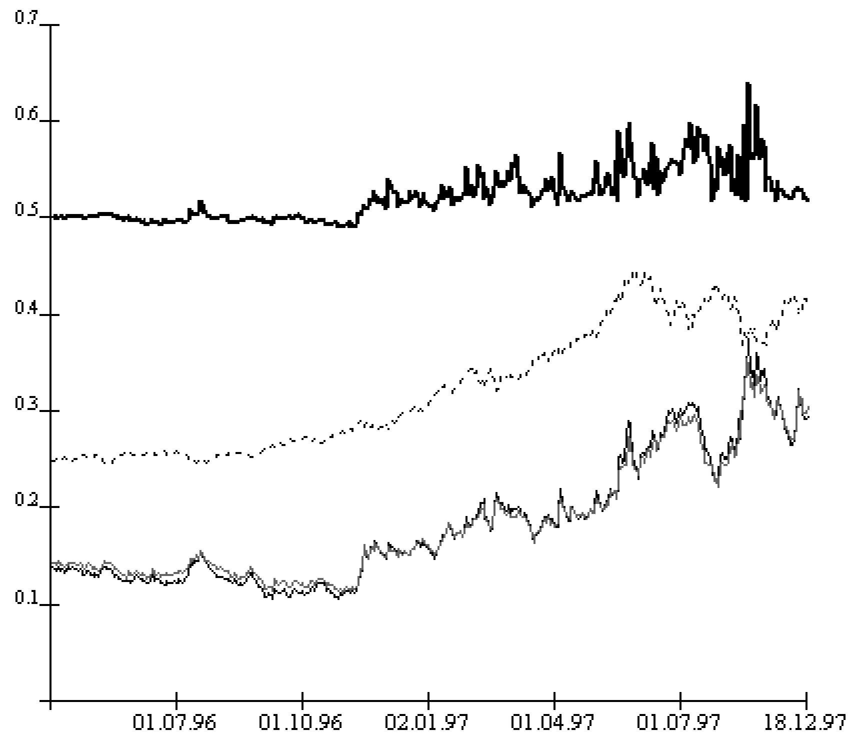

quickly available for market participants either, our ML approach may serve as a good guideline for their daily operations. Still, in order to gauge the empirical performance of the procedure we compute actual exceedances of the ML throughout the sample period, i.e. we compare the actual losses in $t + 1$ of our portfolio and the ML estimated in t. They amount to 12.0% (53 in absolute number), which is less than expected by our modelling approach. We take this as support for the usefulness of ML computations in the sample period under consideration.

7. Concluding Remarks

In this paper we outline a procedure for using principal components analysis to determine the maximum loss of option portfolios bearing vega exposure. The term structure of implied volatilities “at the money” is decomposed into two factors that are used to determine the price sensitivity of ATM DAX options. In the last sections of our paper we propose a parsimonious way of determining the maximum loss of a derivatives portfolio whose primary source of risk is associated with the term structure of implied volatilities. Financial institutions may find our maximum loss approach useful for monitoring the vega exposure of their positions and for setting margin requirements for clients who trade with them.

A stability analysis indicates that the common factors governing implied volatility movements of DAX options may vary over time. It could therefore be interesting to use adaptive approaches to our modelling approach. We leave the topic of adaptive PCA in implied volatility risk management for further research.

REFERENCES

ALEXANDER, C. (2001): "Principals of the skew", RISK, March 2001.

CONT, R. and J. FONSECA (2002): "Dynamics of implied volatility surfaces", Working paper, Ecole Polytechnique, Palaiseau, France.

DERMAN, E. (1999): "Volatility Regimes", RISK, April 1999, 55-59.

FENGLER, M., W. HÄRDLE and CH. VILLA (2001): "Common Principal Components Analysis and the Dynamics of Implied Volatilities", Discussion Paper No. 38, Sonderforschungsbereich 373, Humboldt University Berlin.

HÄRDLE, W. and L. SIMAR (2002): Applied Multivariate Statistical Analysis, Springer Verlag Heidelberg, Heidelberg.

HÄRDLE, W., S. KLINKE and M. MÜLLER (2000): XploRe – The Interactive Statistical Computing Environment, Springer Verlag Heidelberg.

HÄRDLE, W., V. SPOKOINY and G. TEYSSIERE (2000): "Adaptive Estimation for a Time Inhomogeneous Stochastic-Volatility Model", Discussion Paper No. 6, Sonderforschungsbereich 373, Humboldt University Berlin.

REDELBERGER, T. (1994): "Grundlagen und Konstruktion des VDAX-Volatilitätsindex der Deutsche Börse AG", Deutsche Börse AG.

SCHÖNBUCHER, J. (1999): "A Market Model for Stochastic Implied Volatility", Philosophical Transactions of the Royal Society, Series A, Vol. 357, No. 1758, August 1999, 2071-2092.

SKIADOPOULOS, G., S. HODGES and L. CLEWLOW (1999): "The Dynamics of Implied Volatility Surfaces", Review of Derivative Research, 3, 263-282.

STUDER, G. (1995): "Value at Risk and Maximum Loss Optimization", Discussion Paper, ETHZ, RiskLab: Technical Report.

SYLLA, A. and CH. VILLA (2000): Measuring Implied Surface Risk using PCA, in: FRANKE, J., HÄRDLE, W. and STAHL, G. (eds.): Measuring Risk in Complex Stochastic Systems, LNS 147, Springer Verlag, New York, p 131- 147.

TALEB, N. (1997): Dynamic Hedging: Managing Vanilla and Exotic Options, John Wiley, New York.